Author version: Acta Geol. Sinica, vol.85; 2011; 814-825

Spatial distribution and longitudinal variation of clay minerals in the Central Indian Basin

Anil B. Valsangkar

National Institute of Oceanography, Dona Paula, Goa- 400 403, India

Abstract

Grain size and clay mineral distribution up to 45 cm depth in the silty clay sediments from 26 box cores from 10° to 16° S along four longitudes (73.5° to 76.5° E) have been studied for understanding spatial variability in the Central Indian Basin (CIB). It is observed that the average sand content in the basin is 3.8 %, which decreases systematically and longitudinally to 0.3 % towards south. The average illite and chlorite major clay mineral abundance also decrease southwards along the four longitudes from 10° S, and show the limit of influence of the Ganges-Brahmaputra river's supply up to 10° S. However, the average clay content increases from west to east in the basin, and southwards along 73.5° E and either side of 76.5° E fracture zone (fz), which strongly suggests possibility of clay supply due to circulation of Antarctic Bottom Water (AABW) from the south through fz. The distribution of four clay minerals along 73° and 76.5° E fz in the CIB shows dissimilar trends of increase and decrease, and indicate mix environment in the basin. The study indicates that the fz in the CIB have an important role in controlling the distribution of clay minerals.

Key words: Clay minerals, central Indian basin, polymetallic nodules, source, environment.

1 Introduction

The direction of sediment transport in the marine environment is a major concern and the spatial changes in grain size parameters allow the identification of net sediment transport (Pedreros et al., 1996). The complex nature of the sediments and sedimentation processes in the Indian Ocean is thought to be due to the combined effect of an active mid-oceanic ridge system, 90^{o} E aseismic ridge, flexured, folded and faulted nature of the seafloor topography, and uneven supply from the land masses (Heezen and Tharp, 1964; Griffin et al., 1968; Goldberg and Griffin, 1970). Many workers have assigned detrital origin for the of clay mineral assemblages in the sediments of the Indian Ocean (Rateev et al., 1969; Kolla and Biscaye, 1973; Kolla et al., 1976; Rao and Nath, 1988). Most of these studies were based on random surficial samples with low sample density representing large area in the Indian Ocean. The siliceous sediments predominates in the Central Indian Basin (CIB). The northern part of the CIB receives terrigenous influx from the Ganges-Brahmaputra rivers, and the influx is traced up to 8^{o} S (Nath et al., 1989) and 14^{o} S latitudes (Mudholkar et al., 1993). The average sediment accumulation rate in the CIB varies from 1 to 5 mm/ ka (Borole, 1993). The geophysical studies in the CIB have revealed four fracture zones (fz) at 73^{o}, 75.75^{o}, 79^{o} and 83^{o} E (Kamesh Raju et al., 1993). The CIB is also known for rich deposits of polymetallic nodule (PMN) and ferromanganese concretions in the siliceous sediments between 10^{o} and 16^{o} S, and 73^{o} and 76^{o} E, where first generation mining (FGM) area have been allocated by the International Sea Bed Authority (ISBA) after relinquishment (Valsangkar, 2003). Here, the results of clay mineral analysis of 277 sediment sub-samples up to 45 cm depth from 26 box cores stations at 1^{o} spacing from 10^{o} to 16^{o} S latitudes and 73.5^{o} to 76.5^{o} E longitudes covering the PMN allocated area in the CIB are presented. This probably represents the largest systematic study on clay mineralogy of the sediments from the CIB. The present study also corresponds to the initial benthic environmental conditions in the CIB prior to the nodule mining activity in near future. The main objective of this study is to document the systematic changes in the clay mineral abundance in the CIB, and to decipher various deep-sea processes associated with fracture zones controlling these variations.

2 Methodology

The seabed sediments from 26 locations at 1^{o} spacing covering the PMN Pioneer area in the CIB (Figure 1) were obtained using the box corer (with a box of 50 X 50 X 50 cm) during *A.A. Sidorenko* cruise no. 61 (AAS-61). Out of these two stations were in the area designated for FGM. The maximum depth of the sediment core was 45 cm. The siliceous sediments in the box core were sub-sampled at 2 cm interval up to 10 cm depth and at 5 cm interval for remaining length of the box core using a special

device (Valsangkar, 2007). The salt content in the sub-samples was removed in the shore laboratory by repeated washing with Barnstead RO -pure water and the samples were oven dried at 40^{o} C. The sand percentages were determined by wet sieving through a 62 μm sieve, whereas silt (63 to 2 μm) and clays (< 2 μm) were calculated by the standard pipette analysis (Folk, 1968). Recalculated values of the sand-silt-clay fractions were used for preparing triangular plots. Oriented slides of 2 μm size clay fractions were prepared using 1 ml of treated sample for X-ray diffraction (XRD) studies. The measurements were carried out from 3^{o} to 23^{o} at scan speed of 0.05^{o} 2θ per second on the Philips X-ray diffractometer (PW 1840) using Ni filtered Cu Kα radiation, operated at 20 mA and 40 kV. The samples were glycolated and rescanned from 24^{o} to 26^{o}at scan speed of 0.02^{o} 2θ per second after exposing the clay slides to ethylene glycol vapours for 1 hour at 100^{o} C. Typical XRD patterns of the sub-samples from box core 21 are shown in Figure 2. The percentages of dominant clay minerals were determined by weighted peak area method (Biscaye, 1965). The smectite/ illite (S/I) and kaolinite/chlorite (K/C), and kaolinite/ smectite (K/S) ratios were calculated from the respective clay fractions. The smectite crystallinity (V/P) was calculated after Biscaye (1965) by measuring the height of peak above the baseline (P) and the depth of the valley on the low angle of the peak (V), whereas illite crystallinity was calculated after Kitch (1980) by measuring the width (∆2θ) at half peak height at (001) diffraction peak.

3 Results

3.1 Sand

The sand content in the surface sediments from the entire CIB is generally low (up to 2 %), occasionally it exceeds > 5 % and rarely > 10 % (BC-18). The depth profiles show that the sand content increase marginally with depth up to 12^{o} S latitude, and later it remains < 2 % (Figure 3). The average sand content for the entire area for the surface sediments (0-2 cm) is 1.06 % and that for 2-4 cm depth is 1.27 %. Total sand averages for each station are given in Table 1.

3.2 Silt

Silt content in the samples (from surface to ~ 40 cm depth) generally range within 20 to 50 % and more commonly within 20 to 40 %. However, very high (91 to 95 %) and low (7 to 25 %) values of silt were obtained for the deeper sections (10-15 and 30-35 cm respectively) at BC-06. In general, the silt content increases with depth (Figure 4). The surface (0-2 cm) values of silt in the area vary within 20 to 46 % and that for 2-4 cm varies from 25 to 50 %. The average silt content per station is given in Table

1. The average silt content for the surface (0-2 cm; 35 %) and 2-4 cm depth (37 %) sediments in the entire area is similar.

3.3 Clay

The clay content dominates in the area which has range of 44 to 79 % on the surface against the total range from 42 to 81 %. In contrast to sand and silt, the clay content decreases with the depth (Figure 5). The clay averages are given in Table 1. The average clay content in the entire area for the surface is 64 % and that for 2-4 cm depth sections is 62 %. The average clay in the area varies across the latitude and longitude (Table 1).

3.4 Sediment texture (sand-silt-clay ratios)

Although the dominating sediment texture in the area is `silty clay', some sections at few stations are `clayey silt', and `clays' are rare (Table 1). Spatial variations show that `clayey silt' is more common along 12^{o} and 13^{o} S latitude. Similarly, the basin sediments in the west are mostly `silty clay' along 10^{o}, 11^{o} and 14^{o} S latitude.

3.5 Clay mineralogy

Vertical distribution of the clay minerals from 10^{o} to 16^{o} S appears monotonous with depth, amid few changes at places. The major clay mineral in the area (excluding BC-05) is illite, which has wide range (33-71 %), followed by smectite (2-41 %), chlorite (5-37 %) and kaolinite (3-30 %). Kaolinite and chlorite shows nearly equal ranges and smectite commonly shows initial increase up to 10-15 cm. In most stations, kaolinite and chlorite trends are similar and those of illite and kaolinite are opposite (Figure 6, 7). The station averages of smectite, illite, kaolinite and chlorite minerals and their ratio shows spatial variations in the CIB with respect to latitude and longitude (Table 2, 3). The average K/C ratio of clay fractions for a station is quite close to surface value of the respective station, except for BC-05**.** Similarly, the average S/I ratios of clay fractions for the stations between 10^{o} and 13^{o} S are quite close to their surface value, whereas those along 14^{o} and 16^{o} S show deviation from the surface value (Table 3). The average I/S typically decrease along 75.5^{o} and 76.5^{o} fz from 10^{o} to 16^{o} S, whereas decrease of K/S ratios is more pronounced along 75.5^{o} fz (Table 4).

3.6 Crystallinity index

The illite crystallinity shows minor variations (0.1-0.25) with depth. Comparatively, V/P ratios of smectite have large variations (0.1-1.0), which increases with depth for the sampling stations between 13^{o}

and16^{o} S (Figure 8). The averages of illite crystallinity are almost constant in the area, whereas those for smectite show spatial variations (Table 5).

4 Discussion

Spatial variations in the distribution of sand and clay content have been observed in the CIB. Although overall sand content in the basin is low (< 5 %), the sand averages display conspicuous southward decrease along the four longitude from 10^{o} to 16^{o} S, but do not vary along any particular latitude (Table 1). Conversely, the average clay content in the basin increases from 10^{o} to 16^{o} S (southward increase), and also from west to east (lateral increase; Table 1). Further, the average clay content gradually increases from 60 to 70 % particularly along either side of the 76.5^{o} fracture zone (fz; Table 1). Similar small increase in clay is also observed along the 73^{o} fz, but along 74.5^{o} E the clay content decreases from 64 to 55 %. Increase of clay content towards southern latitudes in the CIB therefore suggests additional supply/ source from the south and appears to be locally supported by the volcanic activity. The Northern Central Indian Ridge (NCIR) lacunae (2^{o}-12^{o}S) is also known for the petrographic variations and the influence of Ridge-Transform Interactions (RTI) (Drolia, et al, 2003). Some of the area in the CIB reported to contain fine grained smectite rich sediments derived from the alteration of *in situ* submarine basalts and the associated volcanic products (Kolla and Biscaye, 1976). Although there are no reports of volcanic activity in the CIB on local scale, the presence of seamount and volcanic crater in the study area (NIO, 2009) indicates such possibility in the recent past.

Possibility of contribution from the Rajmahal traps is differed as follows. The Ganges River rises in Himalayas and brings down illite and chlorite (glacial/cold weathering) by eroding Precambrian formations in the higher latitudes and reaches Rajmahal Traps in lower latitudes and ends in West Bengal giving kaolinite and monmorillonite/ smectite (chemical/ warmer weathering). Therefore, contribution from the Rajmahal Traps could have reached to CIB via Bay of Bengal from where the Ganges River ends. In contrast, Subba Rao (1963) found illite and chlorite with minor amount of minormontmorillonite and traces of kaolinite, whereas Rama Murthy and Srivastava (1979) reported illite with minor amounts of kaolinite and montmorillonite (smectite) in the sediments off the Ganges. Rao et al., (1988) further pointed that the Ganges derived sediments does not reach the shelf off the peninsular rivers. In this view, high smectite (>60 %) and kaolinite (< 12 %) in the sediments of western part of the Bay of Bengal reported by Kolla and Biscaye (1973), and Goldberg and Griffin (1970) are derived by the rivers of the southern India, primarily from the Deccan Trap soil. These reports infer that the Ganges (Rajmahal Traps) derived sediment is deposited mostly on the continental shelf or in the

deeper parts of the Bay of Bengal but not towards the southern part. The contribution of smectite and kaolinite coming from the Rajmahal Traps in the CIB sediments is therefore ruled out.

Illite and smectite mineral phases show antipathetic relationships in the CIB. From 10^{o} S to 16^{o} S along either side of 76.5^{o} fz, the average content of illite and chlorite decreases (57 to 43 % and 21 to 18 % respectively, Table 2), whereas those of smectite and kaolinite increases (6-16 % and 17-24 % respectively, Table 2). Similar trend is also depicted from S/I and K/C ratios which show a southward increase (0.1-0.4 and 0.8-1.3 respectively, Table 3). Comparatively, along 73^{o} fz in the western CIB, smectite and illite decrease slightly (16 to 15 %, and 50 to 49 % respectively), and kaolinite and chlorite increase (17 to 18 %, and 16 to 19 % respectively, Table 2). Similarly, along 74.5^{o} E, smectite and kaolinite decreases (15 to 6 %, and 20 to 19 % respectively) whereas, illite and chlorite increases (47 to 49 %, and 17 to 27 % respectively). Dissimilar and opposite trends of the clay minerals (increase or decrease) along four longitudes therefore indicates a mixed environment in the CIB due to different supply sources. However, southward increase of chlorite content along 73^{o} and 74.5^{o} E fz in the CIB reconfirms the earlier observation by Valsangkar and Ambre, 2000, and suggests influence of chlorite rich Antarctic Bottom Water (AABW) in the CIB. Therefore, it is quite likely that the AABW is circulated in the CIB from south to north through the fz.

Previous workers (Siddiquie, 1967; Goldberg and Griffin, 1970) have reported illlite as the predominant clay mineral in the Bay of Bengal sediments and that illite and chlorite are dispersed by turbidity currents from Ganges and Brahmaputra rivers (Kolla and Biscaye, 1973; Kolla and Rao, 1990; Rao and Rao, 1977). The mineralogical and chemical studies have suggested (Nath et al., 1989; Mudholkar et al., 1993; Kolla and Biscaye, 1973) terrigenous influx from the Ganges- Brahmaputra rivers reaching up to 8^{o}, 10^{o}, and 14^{o} S. In the present study, the total averages of smectite (15 %), illite (46 %) kaolinite (21 %) and chlorite (17 %) apparently matche with the sediments of the Ganges Province (> 25-30 illite (up to 70 %) and > 10-12 chlorite; Kolla and Biscaye, 1973). The possibility of the sediments coming from the Australian Province (< 60 % smectite, < 20-25 % illite and > 20 % kaolinite (Kolla and Biscaye, 1973) in to CIB is ruled out due to distinctly different sediment characteristics. Further, gradual decrease (observed in the present study) in the abundance of illite and chlorite mineral phases from 10^{o} to 16^{o} S along 76.5^{o} and to some extent along 73^{o} fz clearly indicates the limit of influence of the Ganges- Brahmaputra rivers up to 10^{o} S. Therefore, it is more likely that the CIB sediments have mid-Indian ridge as a major supply source.

The smectite distribution patterns show large variation in abundance in the CIB. Smectite and kaolinite also being the product of weathering of basic rocks, their average increase from 10^{o} to 16^{o} S (Table 2)

strongly suggests possibility of weathering of basic igneous rocks of the mid-Indian ridge system. Possibility of major supply from the basinal rocks in the CIB appears distant as they exist in very small quantity compared to the sediments. Considering the gradual increase in smectite content along the 76.5^{o} E fz, it appears that considerable amount of smectite abundance may also be related to the 90^{o} E ridge, mid-Indian volcanic or local volcanism along the 76.5^{o} E fz which is a triple junction trace on the Indian plate. The baseline physical conditions of water column (potential temperature, salinity, potential density and the geostrophic circulation regime) studies in the deeper depths in the CIB indicated weak near bottom flow regime chiefly characterized by SW flow bounded by clockwise and anti-clockwise eddies on northern and southern side (Ramesh Babu et al., 2001) also supports the possibility of smectite being brought from the 90^{o} E ridge.

The crystallinity index also supports the view of local source for smectite in the CIB, as the smectite crystallinity averages clearly depict systematic decrease in the south along either side of the 76.5^{o} fz (0.7 to 0.3, and 0.5 to 0.4; Table 5), and an increase along 73^{o} fz and 74.5^{o} E. The opposite trends of smectite increase along two fz therefore point towards two different sources in the CIB. On the country, the illite crystallinity index of illite is less sensitive parameter, which is constant (0.22) for the entire area (Table 5) and indicates only one source. It is observed that the smectite crystallinity is inversely proportional to the smectite abundance (Table 3 and 5). The higher abundance of smectite in the CIB is related to the weathering of basic volcanic rocks provided by the seamounts along the fracture zones. Therefore, the observed variation in smectite crystallinity appears to be due to the varying degree of weathering of basaltic rocks in the CIB.

5 Conclusions

The clay mineralogical studies on the CIB sediments show that silty clay sediments are more abundant than the clayey silt, and although, sand content is less than 2 %, the averages decrease towards southern latitudes. Vertical profiles show increase of sand and silt content, and decrease of clay with depth. Gradual increase in the clay content along either side of the 76.5^{o} fracture zone in the CIB suggests additional source of supply. This observation is further supported due to the increase of the smectite crystallinity along 73.5^{o} fz and 74.5^{o} E, and decrease along both side of 76.5^{o} E fz. The observed variations in the smectite crystallinity is probably due to the varying degree of weathering of volcanic basalts in the CIB.

The illite and chlorite clay minerals in the CIB decrease systematically towards southern latitudes and indicates the influence of the Ganges- Brahmaputra rivers up to 10^{o} S. Illite and smectite mineral

phases show antipathetic relationships in the CIB and depict dissimilar and opposite trends along 73° and 76.5° fz and 74.5° E longitude indicating mix environment. Increase in the smectite content along the 76.5° E fz in the CIB strongly indicates the possibility of smectite coming from 90° E ridge, mid-Indian volcanic or local volcanism along the 76.5° E fz. The two fz in the CIB therefore appears to control the distribution of four clay minerals. The data further suggests that the AABW is channeled in the CIB through the fz.

Acknowledgements

Financial support provided by the D.O.D. and MoES, New Delhi, under the project, `Environmental Impact Assessment studies of nodule mining' is gratefully acknowledged. In house laboratory assistance by Ms Domnica Fernandes is highly appreciated. Mr. Jai Sankar and R. Uchil are thanked for preparing the sample location map. Mr. G.A. Prabhu is thanked for the XRD work .This is NIO (CSIR) contribution no.---.

References

Biscaye, P.E., 1965. Mineralogy and sedimentation of recent deep sea clay in Atlantic Ocean and adjacent seas and oceans. *Bull. Geol. Soc. Amer.,* 76: 803-831.

Borole, D.V. 1993. Late Pleistocene sedimentation: A case study of the Central Indian Ocean Basin. *Deep-Sea Res*. (A), 40 (4): 761-775.

Drolia, R.K., Iyer, S.D., Chakraborty, B., Kodagali, V.N., Ray D., Misra, S., Andrade, R., Sarma, K.V.L.N.S., Rajasekhar, R.P., and Mukhopadhyay, R., 2003. The Northern Central Indian Ridge: Geology and tectonics of fracture zones-dominated spreading ridge segments, *Curr. Sci.*, 85 (3): 290-298.

Folk, R.L., 1968. Petrology of sedimentary rocks. University of Texas, Austin, Texas, 170.

Goldberg, E.D., and Griffin, J.J., 1970, The sediments of the northern Indian Ocean, *Deep-Sea Res*., 17: 513-537.

Griffin, J.J., Windom, H., and Goldberg, E.D., 1968. The distribution of clay minerals in the world ocean. *Deep-Sea Res*., 15: 433-459.

Heezen, B.C., and Tharp, M., 1964. Physiographic diagram of the Indian Ocean, the Red Sea, the South China Sea, the Sulu Sea and Celebes Sea. *Geol. Soc. Am.,* Scale: 1:11x10^6.

Kamesh Raju, K.A., Ramprasad, T., Kodagali, V.N., and Nair, R.R., 1993. Multibeam bathymetric, gravity and magnetic studies over 79^{o} E fracture zone, Central Indian Basin. *J. Geophys. Res.*, 98 (B6): 9605-9618.

Kitch, H.J., 1980. Incipient metamorphism of Cambro-Silurian clastic rocks from the Jámtland Supergroup, Central Scandinavian Caledonides, Western Sweden: illite crystallinity and `vitrinite' reflectance. *J. Geol. Soc. Lond.,* 137: 271-288.

Kolla, V., and Biscaye, P.E., 1973. Clay mineralogy and sedimentation in the eastern Indian Ocean. *Deep-Sea Res.*, 20: 727-738.

Kolla, V., Henderson, L., and Biscaye., P. E., 1976. Clay mineralogy and sedimentation in the western Indian Ocean. *Deep-Sea Res.,* 23: 949–961.

Kolla, V., and Rao, N.M., 1990. Sedimentary sources in the surface and near- surface sediments of Bay of Bengal. *Geo-Mar. lett.,* 10: 129-136.

Mudholkar, A.V., Pattan, J.N., and Parthiban, G., 1993. Geochemistry of deep-sea sediment cores from the Central Indian Ocean Basin. Indian J. Mar. Sci., 22(4): 241-246.

NIO, 2009. Report on the 38th Oceanographic cruise of *RV Academik Boris Petrov* (07 Sept.–07Oct., 2009), National Institute of Oceanography, Dona Paula, Goa, 56.

Nath, B.N., Rao, V.P., and Becker, K.P., 1989. Geochemical evidence of terrigenous signature influence in deep-sea sediments up to 8^{o} S in the Central Indian basin. *Mar. Geol.,* 87: 301-313.

Pedreros, R., Howa, H. L., and Michel, D., 1996. Application of grain size trend analysis for the determination of sediment transport pathways in intertidal areas. *Mar. Geol.,* 135: 35–49.

Rama Murthy, M., and Srivastava, P.C., 1979. Clay minerals in the shelf sediments of the northwestern part of the Bay of Bengal. *Mar. Geol.*, 33: M21-M32.

Ramesh Babu, V., Suryanarayana, A., and Murty, V.S.N., 2001. Thermohaline circulation in the Central Indian Ocean Basin (CIB) during austral summer and winter periods of 1997. *Deep-Sea Res. II,* 48(16): 3327-3342.

Rao, N.V.N.D., and Rao, M.P., 1977. Clay mineral distributuin in sediments of the eastern part of Bay of Bengal. *Indian J. Mar. Sci*., 6, 166-168.

Rao, V.P., and Nath B.N., 1988. Nature, distribution and origin of clay minerals in grain size fractions of sediments from manganese nodule field, Central Indian Basin. *Indian J. Mar. Sci*., 17: 202-207.

Rao, V.P., Reddy, N.P., and Rao, Ch. M., 1988. Clay mineral distribution in the shelf sediments off the northern parts of the east coast of India. *Cont. Shelf Re*s.*,* 8 (2), 145-151.

Rateev, M.A., Gorbunova, Z.N., Lisitzin, A.P., and Nosov, G.L., 1969. The distribution of clay minerals in the ocean. *Sedimentol.*, 13: 21-43.

Siddiquie, H.N., 1967. Recent sediments of the Bay of Bengal. *Mar. Geol,* 5: 249-291.

Subba Rao, M., 1963. Clay mineral composition of shelf sediments off the east coast of India. *Proc. Indian Acad. Sci.*, A, 58: 6-15.

Valsangkar, A.B., 2003. Deep-sea polymetallic nodule mining: Challenges ahead for technologists and environmentalists. *Mar. Georesour. Geotechnol.*, 21(2): 81–91.

Valsangkar, A.B., 2007. A device for finer-scale sub-sectioning of aqueous sediments. *Curr. Sci.,* 92(4): 428-431.

Valsangkar, A.B., and Ambre, N.V., 2000. Distribution of grain size and clay minerals in the sediments from the INDEX area, Central Indian Basin. *Mar. Georesour. Geomor.,* 18(3): 189-199.

List of Tables

List of figures

Table 1. Average sand, silt, clay content and major sediment texture in the CIB

Lat.	Sand %				Silt %				Clay %				Sediment texture*			
(^{o}S).	73.5^0	74.5^0	75.5^0	76.5^0 E	73.5^0	74.5^0	75.5^0	76.5^0 E	73.5^0	74.5^0	75.5^0	76.5^0 E	73.5^0	74.5^0	75.5^0	76.5^0 E
10			N.D.	2.18			N.D.	36.07			N.D.	61.75			Sc	Sc+Cs
11	3.80	2.00	N.D.	2.00	39.96	34.21	N.D.	31.54	56.24	63.79	N.D.	66.46	Sc	Sc	Sc+Cs	Sc+Cs
12	2.91	1.37	1.68	2.36	37.78	40.89	41.08	30.42	59.31	57.75	57.25	67.23	Sc+Cs	Sc+Cs	Sc+Cs	Sc
13	1.15	3.05	4.13	2.04	46.54	37.88	36.74	48.65	52.31	59.07	60.13	49.31	Sc+Cs	Sc+Cs	Sc+Cs+Cl	Sc+Cs
14	1.85	1.58	1.93	1.28	38.05	39.87	35.72	32.67	60.11	58.55	62.35	66.05	Sc	Sc+Cs	Sc	Sc
15	0.76	0.43	1.37	2.35	39.84	40.75	46.19	34.96	59.41	58.83	52.44	62.88	Sc+Cs	Sc	Sc+Cs	Sc+Cl
16	1.27	0.62	1.50	0.30	44.18	44.32	30.67	26.87	54.55	55.06	67.83	72.83	Sc+Cs	Sc+Cs	Sc	Sc

N.D.= No data; Sc= Silty clay, Cs= Clayey silt, Cl= Clay

Table 2. Averages of clay minerals in the CIB

Lat.	Smectite %				Illite %				Kaolinlite %				Chlorite %			
(^{o}S).	73.5^0	74.5^0	75.5^0	76.5^0 E	73.5^0	74.5^0	75.5^0	76.5^0 E	73.5^0	74.5^0	75.5^0	76.5^0 E	73.5^0	74.5^0	75.5^0	76.5^0 E
10			N.D.	5.56			N.D.	56.65			N.D.	16.61			N.D.	21.18
11	16.47	15.49	N.D.	9.82	50.42	47.38	N.D.	54.86	17.19	20.22	N.D.	16.55	15.97	16.98	N.D.	18.77
12	N.D.	18.63	10.64	10.66	N.D.	46.24	50.90	51.55	N.D.	17.98	20.25	20.67	N.D.	17.16	18.52	17.17
13	13.02	11.63	11.79	8.56	54.33	48.39	48.76	50.88	17.06	23.29	21.74	22.35	15.58	16.70	17.71	18.22
14	12.35	14.24	13.48	28.50	47.74	49.36	43.42	34.12	21.40	19.26	23.15	21.91	18.51	17.14	19.95	15.47
15	14.37	14.55	13.54	13.87	47.34	49.31	46.35	47.40	18.26	19.39	21.74	19.22	20.03	16.75	18.37	19.51
16	14.69	6.46	24.92	15.75	48.82	47.05	45.32	42.65	17.94	19.36	16.51	23.69	18.55	27.12	13.24	17.90

N.D.= No data

Table 3. Averages of S/I and K/C ratio in the CIB

Lat.	S/I ratio (average)				S/I ratio (surface)				Average K/C ratio				Surface K/C ratio			
(°S).	73.5°	74.5°	75.5°	76.5° E	73.5	74.5	75.5	76.5° E	73.5°	74.5°	75.5°	76.5° E	73.5	74.5	75.5	76.5° E
10			N.D.	0.10			N.D.	0.06			N.D.	0.81			N.D.	0.88
11	0.33	0.33	N.D.	0.19	0.20	0.40	N.D.	0.20	1.09	1.20	N.D.	0.91	1.00	1.33	N.D.	1.33
12	N.D.	0.41	0.21	0.21	N.D.	0.46	0.17	0.19	N.D.	1.05	1.10	1.22	N.D.	1.00	1.00	0.90
13	0.24	0.36	0.26	0.17	0.25	0.08	0.11	0.18	1.11	0.35	1.25	1.24	1.00	1.17	1.29	1.00
14	0.28	0.29	0.33	0.93	0.50	0.34	0.15	0.36	1.20	1.21	1.16	1.57	1.40	2.40	1.22	2.43
15	0.31	0.32	0.31	0.29	0.50	0.46	0.22	0.21	1.12	0.92	1.21	1.01	1.12	1.11	1.22	0.86
16	0.31	0.15	0.58	0.38	0.13	0.39	0.38	0.21	1.03	0.72	1.29	1.34	0.89	0.79	1.14	1.00

N.D.= No data

Table 4. Averages of I/S and K/S ratio in the CIB

Lat.	I/S ratio (average)				% of I in I/S ratio				K/S ratio (average)				% of K in K/S ratio			
(°S).	73.5°	74.5°	75.5°	76.5° E	73.5	74.5	75.5	76.5° E	73.5°	74.5°	75.5°	76.5° E	73.5	74.5	75.5	76.5° E
10			N.D.	10.19			N.D.	5.77			N.D.	2.99			N.D.	0.50
11	3.06	3.06	N.D.	5.59	1.54	1.45	N.D.	3.06	1.04	1.31	N.D.	1.69	0.18	0.26	N.D.	0.28
12	N.D.	2.48	4.78	4.84	N.D.	1.15	2.43	2.49	N.D.	1.69	1.90	1.94	N.D.	0.30	0.39	0.40
13	4.17	4.16	4.14	5.94	2.27	2.01	2.02	3.02	1.31	2.00	1.84	2.61	0.22	0.17	0.40	0.58
14	3.86	3.47	3.22	1.20	1.84	1.71	1.40	0.41	1.73	1.35	1.72	0.77	0.37	0.26	0.40	0.17
15	3.29	3.39	3.42	3.41	1.56	1.67	1.59	1.62	1.27	1.33	1.61	1.39	0.23	0.26	0.35	0.27
16	3.30	7.28	1.82	2.71	1.61	3.43	0.82	1.15	1.22	3.00	0.66	1.50	0.22	0.58	0.11	0.36

N.D.= No data

Table 5. Average smectite and illite crystallanity in the CIB

Lat.	Smectite crystallanity				Illite crystallanity			
(°S).	73.5°	74.5°	75.5°	76.5° E	73.5°	74.5°	75.5°	76.5° E
10			N.D.	0.74			N.D.	0.22
11	0.32	0.31	N.D.	0.61	0.20	0.20	N.D.	0.21
12	N.D.	0.23	0.50	0.48	N.D.	0.20	0.20	0.22
13	0.39	0.40	0.45	0.52	0.20	0.20	0.20	0.20
14	0.44	0.42	0.43	0.40	0.20	0.20	0.20	0.19
15	0.48	0.43	0.43	0.41	0.20	0.20	0.20	0.21
16	0.46	0.53	0.43	0.34	0.21	0.20	0.20	0.22

N.D.= No data

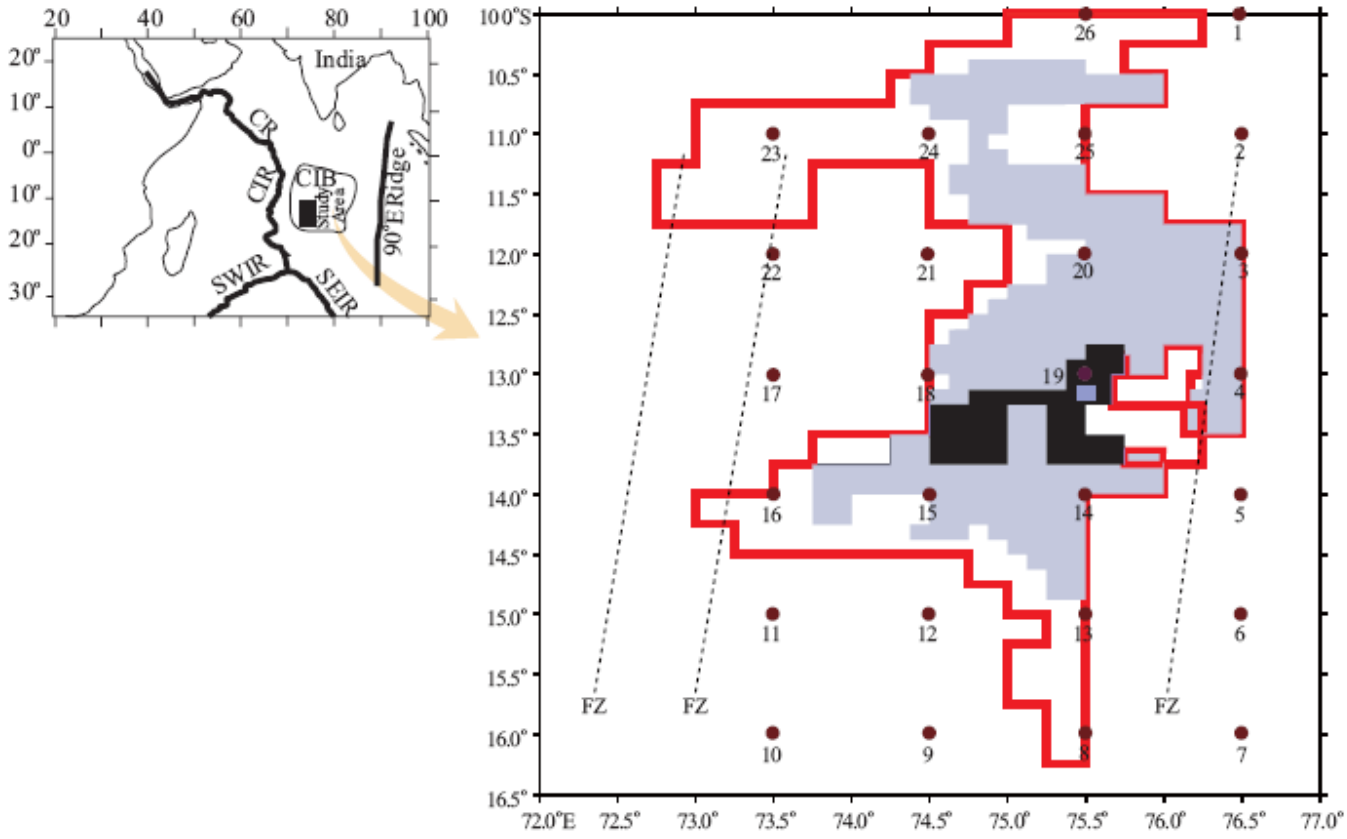
20
40
60
80
100
20°
10°
0°
10°
20°
30°
India
CR
CIR
CIB
Study Area
90°E Ridge
SWIR
SEIR
100°S
10.5°
11.0°
11.5°
12.0°
12.5°
13.0°
13.5°
14.0°
14.5°
15.0°
15.5°
16.0°
16.5°
72.0°E
72.5°
73.0°
73.5°
74.0°
74.5°
75.0°
75.5°
76.0°
76.5°
77.0°
FZ
FZ
FZ

Fig.1.

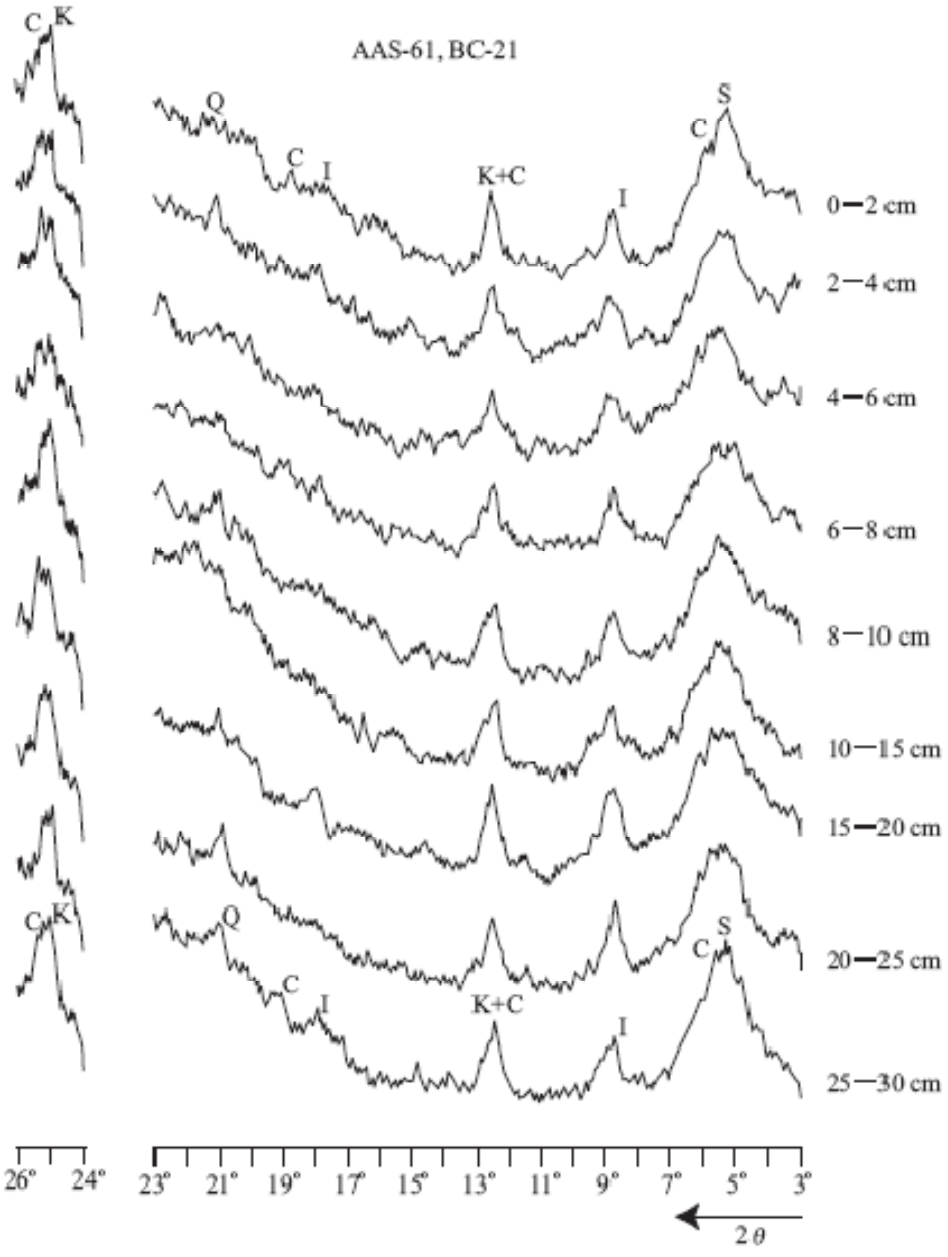
AAS-61, BC-21
C K
Q
C
I
K+C
I
C
S
0—2 cm
2—4 cm
4—6 cm
6—8 cm
8—10 cm
10—15 cm
15—20 cm
20—25 cm
25—30 cm
C K
Q
C
I
K+C
I
C
S
26° 24° 23° 21° 19° 17° 15° 13° 11° 9° 7° 5° 3°
2θ

Fig.2.

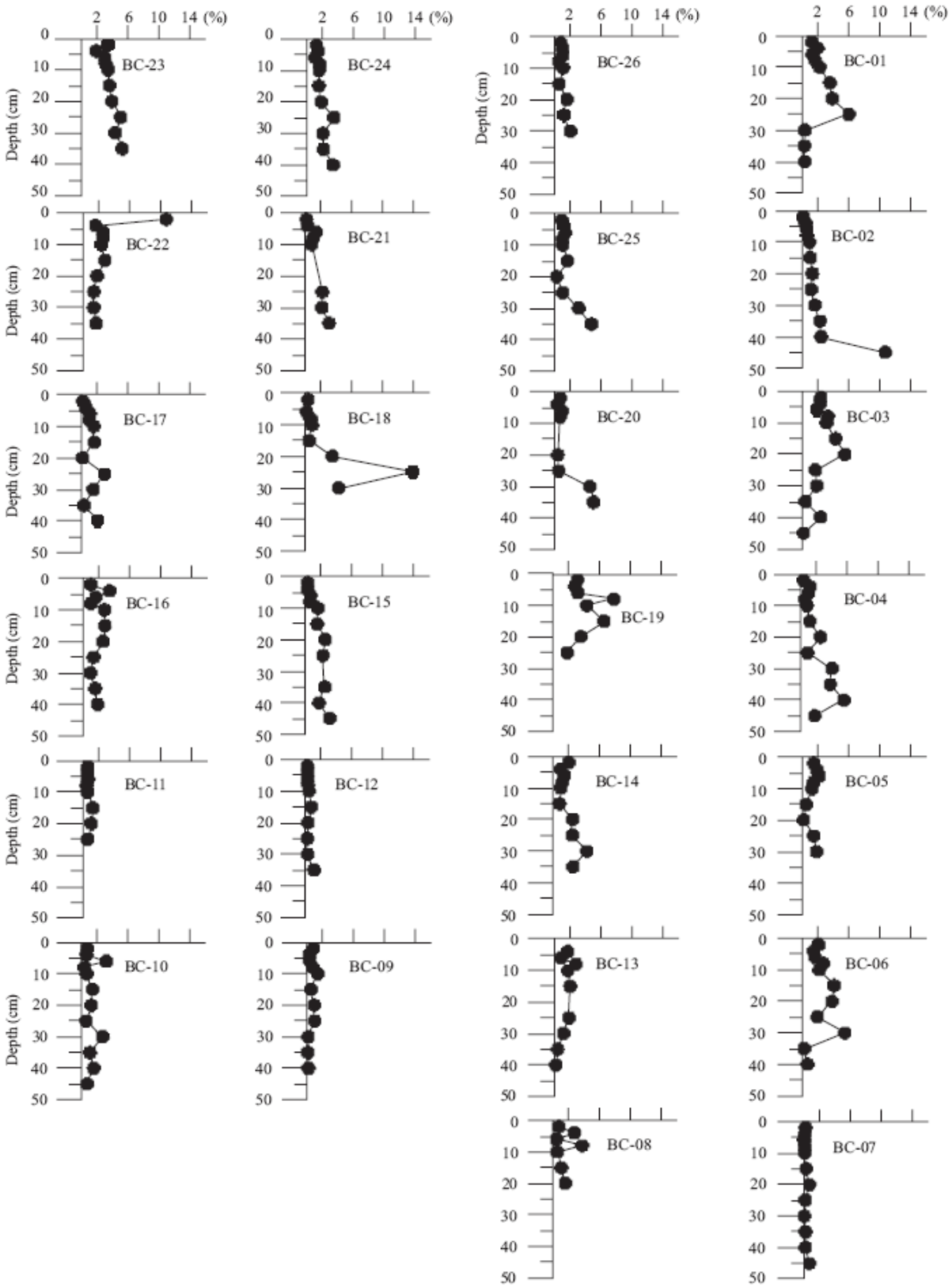
2 6 10 14 (%)
Depth (cm)
0 10 20 30 40 50
BC-23
BC-24
BC-26
BC-01
BC-22
BC-21
BC-25
BC-02
BC-17
BC-18
BC-20
BC-03
BC-16
BC-15
BC-19
BC-04
BC-11
BC-12
BC-14
BC-05
BC-10
BC-09
BC-13
BC-06
BC-08
BC-07

Fig.3.

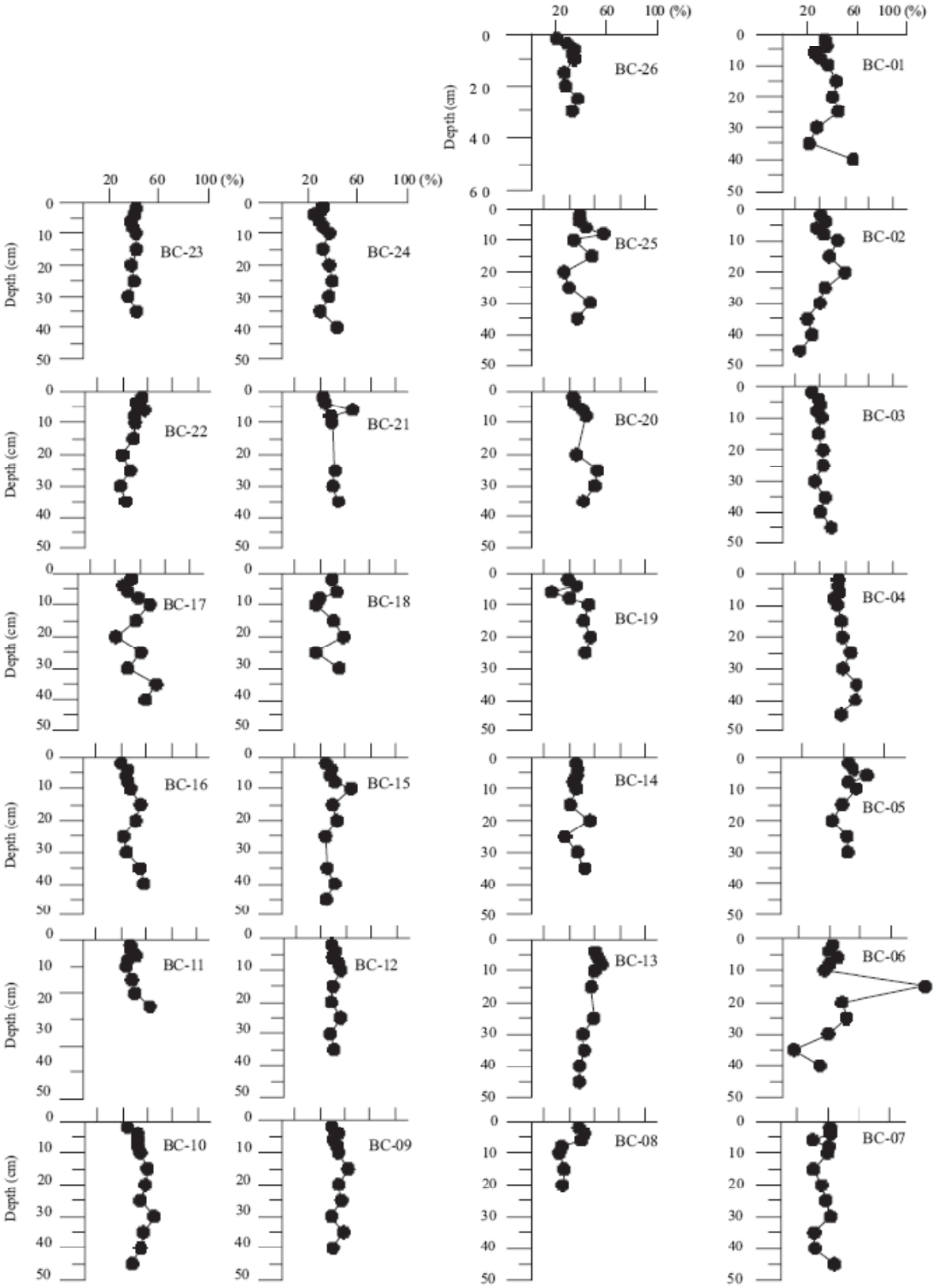
20 60 100 (%)
Depth (cm)
0 10 20 30 40 50
BC-23
BC-24
BC-26
BC-01
BC-22
BC-21
BC-25
BC-02
BC-20
BC-03
BC-17
BC-18
BC-19
BC-04
BC-16
BC-15
BC-14
BC-05
BC-11
BC-12
BC-13
BC-06
BC-10
BC-09
BC-08
BC-07

Fig. 4.

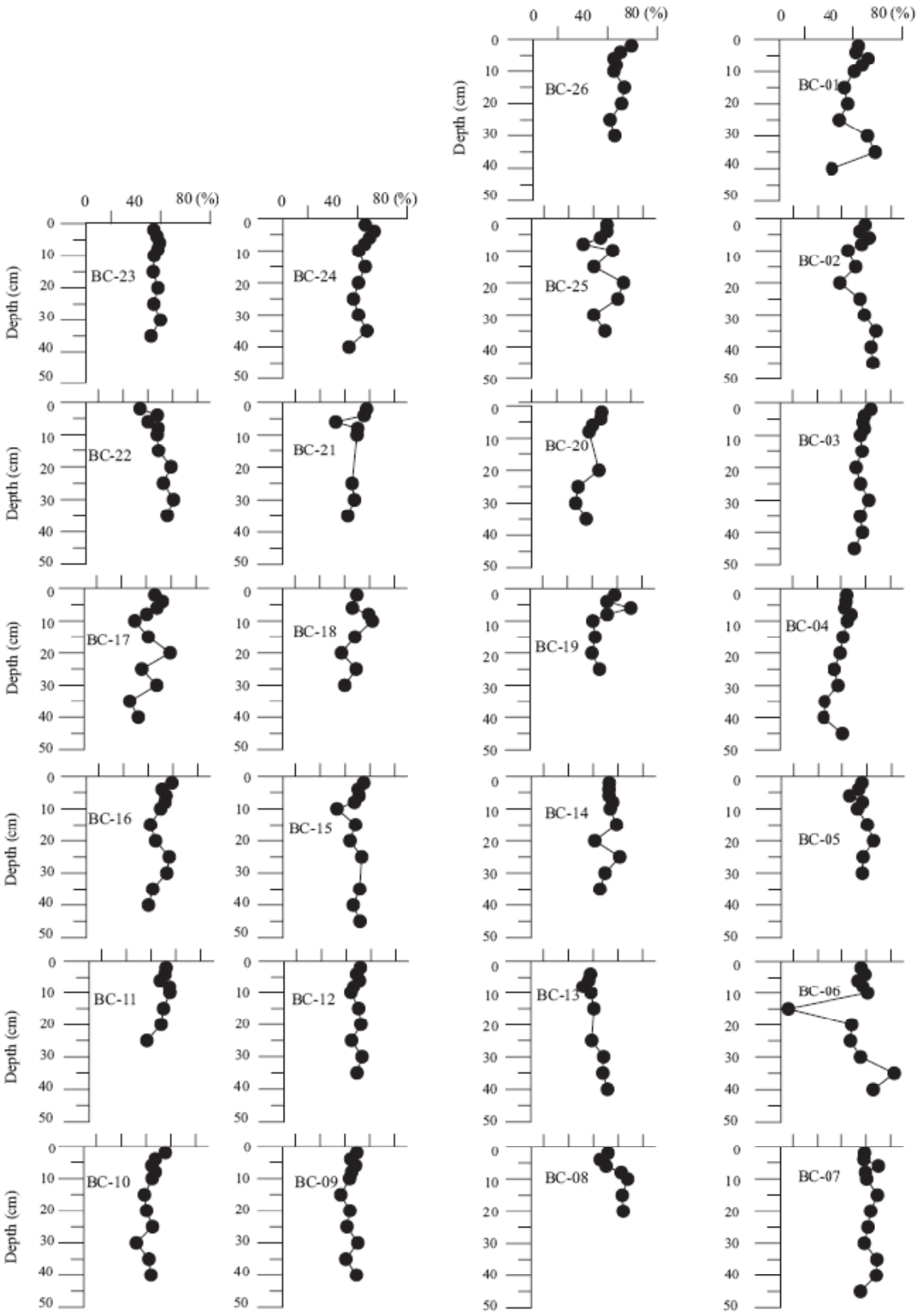
0 40 80 (%)
Depth (cm)
0 10 20 30 40 50
BC-23
BC-24
BC-26
BC-01
BC-22
BC-21
BC-25
BC-02
BC-20
BC-03
BC-17
BC-18
BC-19
BC-04
BC-16
BC-15
BC-14
BC-05
BC-11
BC-12
BC-13
BC-06
BC-10
BC-09
BC-08
BC-07

Fig.5.

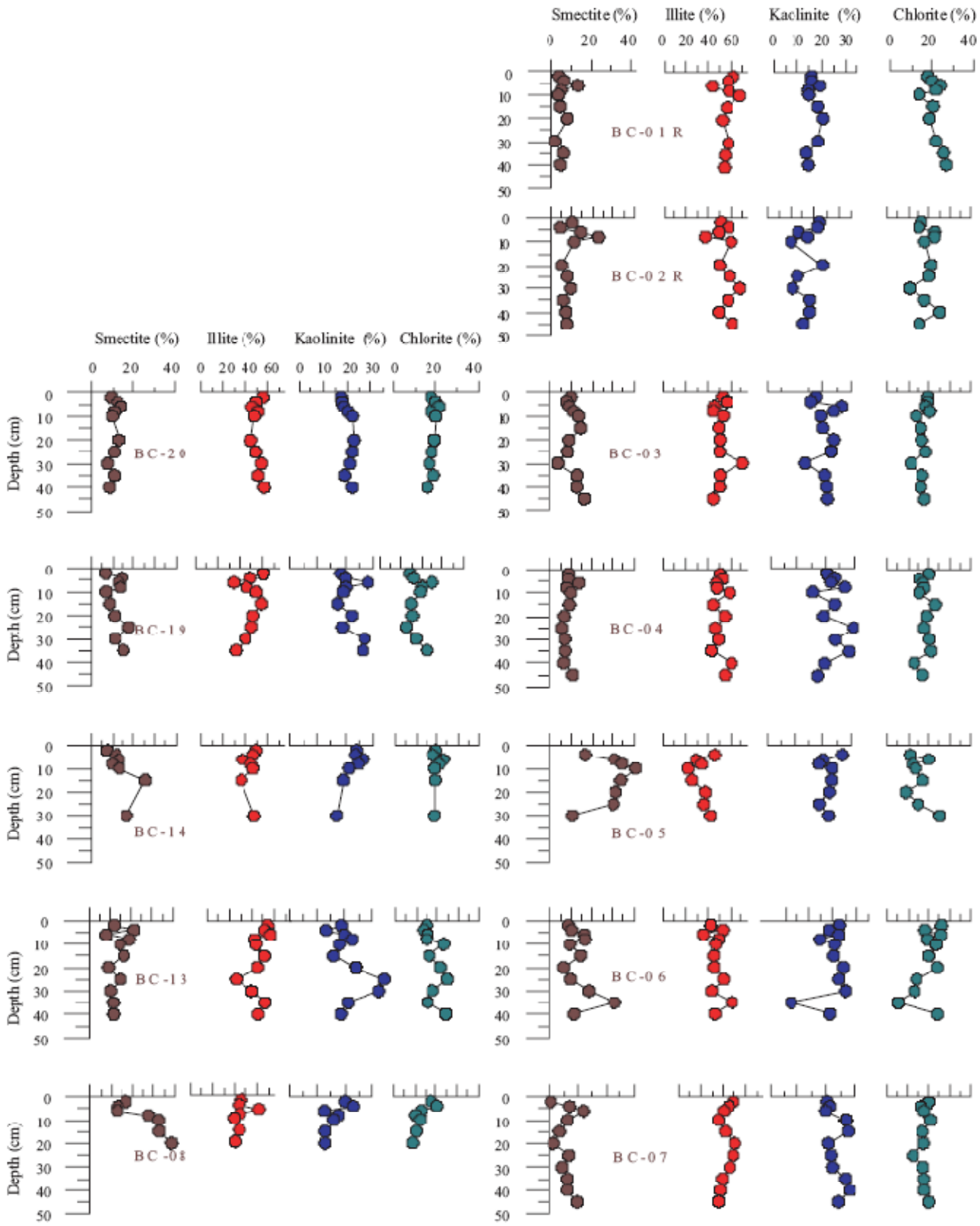
Smectite (%)
Illite (%)
Kaclinite (%)
Chlorite (%)
Kaolinite (%)
Depth (cm)
BC-01R
BC-02R
BC-20
BC-03
BC-19
BC-04
BC-14
BC-05
BC-13
BC-06
BC-08
BC-07

Fig.6.

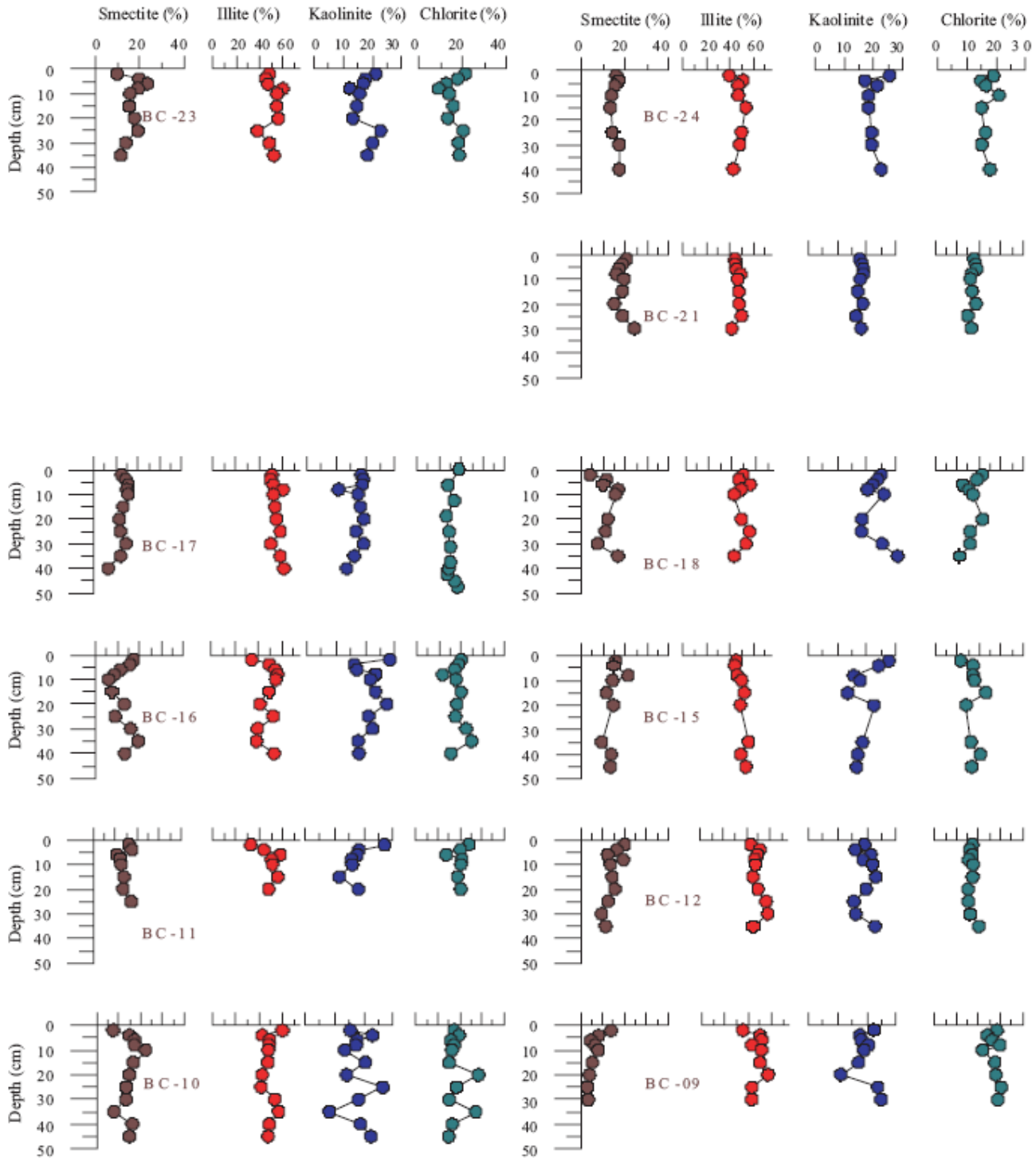
Smectite (%)
Illite (%)
Kaolinite (%)
Chlorite (%)
Depth (cm)
BC -23
BC -24
BC -21
BC -17
BC -18
BC -16
BC -15
BC -11
BC -12
BC -10
BC -09

Fig.7.

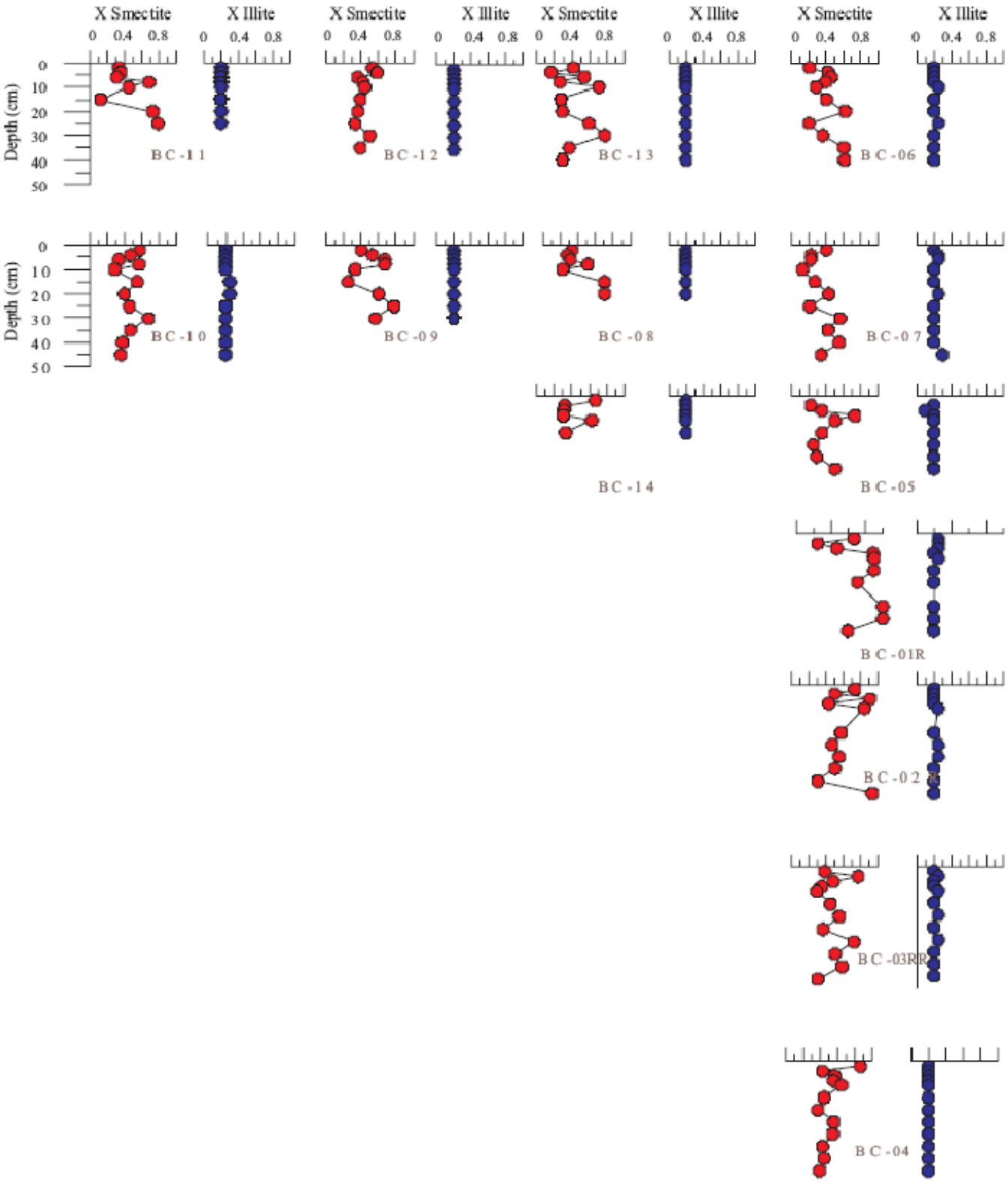
X Smectite
X Illite
0 0.4 0.8
Depth (cm)
0
10
20
30
40
50
BC-11
BC-12
BC-13
BC-06
BC-10
BC-09
BC-08
BC-07
BC-14
BC-05
BC-01R
BC-02
BC-03RR
BC-04

Fig.8.